Theor Chim Acta (1991) 78: 211–230

Theoretica Chimica Acta

Stationary points on the aminomethanol potential energy surface

B. D. El-Issa and R. N. Budeir
Chemistry Department, Kuwait University, P.O. Box 5969, 13060 Safat, Kuwait

Received February 5, 1990; received in revised form May 25, 1990/Accepted June 1, 1990

Summary. In this work we study surface fitting equations for a rigid rotor model of aminomethanol. The energies were obtained from the GAUSSIAN88 package using 3-21G bases and fitted on a least square equation, thus generating a Fourier series expansion of the energy as a function of two dihedral angles. The dihedral angles chosen are those that represent rotation around the C–O and N–C axes in the first case, and rotation around C–O and inversion around the amino group in the second case. Results indicate that the hydroxyl hydrogen is subject to almost free rotation around the C–O axis. Further fully relaxed 6-31G* calculations were performed in order to qualify the results obtained for the rigid rotor model.

Key words: Aminomethanol – Internal rotations – Potential energy surface – Stationary points

1. Introduction

The identification of critical points on a potential energy surface is not straightforward and requires a proper description of the curvature around these points. The surface obtained from the variation of the total energy with two internal coordinates may, however, lead to a situation in which minima, transition states and maxima [1] can be approximated.

The total energy of a rigid rotor, for instance, may conveniently be obtained from single point *ab initio* calculations for a given set of two internal coordinates q_1 and q_2. In as much as rigid rotors are approximate models, it has been shown by various authors that it is not necessary to re-optimize the structure for a given conformer in order to obtain an overall topological picture of the surface [2–4]. In addition, low level STO-3G *ab initio* single point calculations have been shown to produce results that are capable of reproducing the changes that are incurred upon variation of the dihedral angles [2, 5, 6]. Davidson et al. [7] have actually reported singlet and triplet rotational potential surface studies on dihydroxycarbene using STO-3G, DZ and DZP bases and were able to show that π electron donation is mainly responsible for the stability of the ground state singlet.

In general, if one were able to fit the total energy and the two coordinates q_1 and q_2 on surface equations, the gradient of such an energy and the corresponding Hessian matrix would make it possible for one to identify all the critical points correctly. The energy in this case would be given by [3, 8]

$$E(q_1, q_2) = k + \sum_{i=1}^{m} c_i f_{1i}(q_1) f_{2i}(q_2), \tag{1}$$

in which k is a constant, f_{1i} and f_{2i} correspond to the ith fitted function of q_1 and q_2, respectively and c_i is an appropriate constant that premultiplies the ith term in the linear expansion. The ith functions f_{1i} and f_{2i} are normally periodic or exponential functions, depending on whether the coordinates describe rotation of dihedral angles or elongation of bonds. The above equation may be conveniently written as

$$E(q_1, q_2) = k + \text{Trace}(\tilde{\boldsymbol{C}}\tilde{\boldsymbol{F}}), \tag{2}$$

in which $\tilde{\boldsymbol{F}}$ is matrix given by

$$\tilde{\boldsymbol{F}} = |f_1\rangle\langle f_2|, \tag{3}$$

where $|f_1\rangle$ is a column vector that contains the fitted function for variable q_1 and $\langle f_2|$ is a row vector that contains the corresponding function for variable q_2. The matrix $\tilde{\boldsymbol{C}}$ is obviously a diagonal matrix, the elements of which constitute the coefficients c. At the kth critical point, the following holds

$$\left(\frac{\partial \text{Trace}(\tilde{\boldsymbol{C}}\tilde{\boldsymbol{F}})}{\partial q_1}\right)_{q_1 = q_{1k}} = \left(\frac{\partial \text{Trace}(\tilde{\boldsymbol{C}}\tilde{\boldsymbol{F}})}{\partial q_2}\right)_{q_2 = q_{2k}} = 0. \tag{4}$$

The Hessian matrix evaluated at this point ($\tilde{\boldsymbol{H}}_k$), is given by

$$\tilde{\boldsymbol{H}}_k = \begin{pmatrix} t_k^{11} & t_k^{12} \\ t_k^{21} & t_k^{22} \end{pmatrix}, \tag{5}$$

in which

$$t_k^{ij} = \left(\frac{\partial^2 \text{Trace}(\tilde{\boldsymbol{C}}\tilde{\boldsymbol{F}})}{\partial q_i \, \partial q_j}\right)_{q_i = q_{ik},\, q_j = q_{jk}}. \tag{6}$$

Noting that the above Hessian is Hermitian, it is straightforward to show that the corresponding eigenvalues at the kth critical point, a_k, are given by

$$a_k = \frac{(t_k^{11} + t_k^{22}) \pm \sqrt{(t_k^{22} - t_k^{11})^2 + 4(t_k^{12})^2}}{2}. \tag{7}$$

The quadratic dependence of the total energy on two internal coordinates leads to a simple equation that, in turn, results in an approximate description of minima, transition states and maxima. The coordinates that define the critical points may then be used as a starting point for a search of the corresponding points using *ab initio* methods. In the case of hypersurface and higher order surface equations, the eigenvalues of the Hessian may be determined appropriately by updating the Hessian [9] using available techniques, such as the Davidon et al. [10], Murtagh and Sargent [11] and the Broyden et al. [12] methods.

2. Method

The GAUSSIAN88 package [13] at the 3-21G level of approximation was used for the single point evaluation of the energy of aminomethanol. Program STEPWISE [14] was used to fit the GAUSSIAN88 points on a surface equation by a least square method. For the identification of the critical points, we have used the program VA05 [15] and the GAUSSIAN88 package. Two surface equations were generated, the first upon the variation of the two dihedral angles θ_1 and θ_2 (herefrom referred to as the (θ_1, θ_2) surface) and the second upon variation of the dihedral angles θ_1 and γ (herefrom referred to as the (θ_1, γ) surface) (Diagram 1).

The angle θ_2 defines the dihedral angle that the vector perpendicular to that defining the lone pair of electrons on N makes with the N–C–O plane.Thus the point $\theta_2 = 0.0°$ corresponds to the case in which the lone pair of electrons is antiperiplanar with respect to the N–C–O plane. A rigid rotor model was used in which all the angles were chosen to be tetrahedral and in which the following bond lengths were used: $r_{OH} = 0.9661$ Å; $r_{CO} = 1.4457$ Å; $r_{CH} = 1.0807$ Å; $r_{CN} = 1.4350$ Å and $r_{NH} = 0.9956$ Å. Aminomethanol has been chosen because it presents a case in which rotational energy barriers around the C–N and C–O bonds can be studied in relation to the energy barriers involved in inversion about the amino group. The molecule, in essence, mimics aminosulfonic acid and N-sulfates which are essential for the biological activity of mucopolysaccharide Heparin [16, 17] for which little is known about the rotational energy barriers around the S–O and S–N bonds. *Ab initio* studies on O-sulfated systems [18] have been reported and barriers to internal rotation around the S–O bonds were found to be minimal.

The three- and two-dimensional surface plots were drawn using program KUGRAPHICS [19]. The average time required to perform a single point calculation was 3 minutes on a VAX8820. The SCAN option of the GAUSSIAN88 package was used to sweep dihedral angles. In the case of the (θ_1, θ_2) surface, θ_2 was held at 0.0° while θ_1 was varied from 0.0° to 360.0° in 5.0° increments. The same sweep was repeated by incrementing the θ_2 angle by 60.0°. This was necessary since an increment of 120.0° for θ_2 produced poor fits along the θ_2 axis. Using these variations, the curvatures on the surface were reproduced with reasonable accuracy.

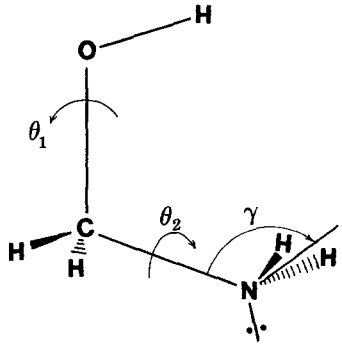

Diagram 1.

3. Results and discussion

3.1. The (θ_1, θ_2) *surface*

In Fig. 1a the difference between the 3-21G single point energy and the lowest energy structure in kcal/mol is plotted against the dihedral angle θ_2 for a fixed value of θ_1 equal to 0.0°. The lowest energy structure for this system occurs at the coordinate ($\theta_1 = 0.0°, \theta_2 = 0.0°$) and is calculated to be -169.0858331 hartrees. The system is seen to exhibit reflective symmetry about the point $\theta_2 = 180.0°$. Figure 1b is a similar representation in which θ_1 is fixed at 180.0°. The lowest energy structure in this case occurs at the point (180.0°, 0.0°) and is calculated to be -169.0903680 hartrees. Although the symmetry is retained in these two rigid rotors, it is apparent that if θ_1 assumed any other values, the symmetry around the $\theta_2 = 180.0°$ point will break down. The figures are actually two-dimensional entities and the apparent critical points are not true stationary points on the surface since θ_1 is not allowed to relax upon the variation of θ_2. We therefore report stationary points on these figures in terms of (θ_1, θ_2) that are obtained after optimizing the two angles to a stationary point and then performing a frequency calculation in order to correctly identify these points as either minima (*m*), maxima (*M*) or transition states (*S*). In Fig. 1a we identify two unique transition states that occur at the points (0.0°, 0.0°) and (0.0°, 180.0°). The point identified as *M*1 is a local maximum and when optimized at the 3-21G level occurs at (11.95°, 63.34°). The two unique points (180.0°, 0.0°) and (180.0°, 180.0°) are identified respectively as *m*9 and *S*5, as shown in Fig. 1b.

In Figs. 1c and 1d, we display plots in which θ_2 is fixed at 0.0° and 180.0°, respectively, and in which θ_1 is varied from 0.0° to 360.0° by increments of 5.0°. The topologies of these surfaces are appreciably different from those considered earlier and the reflection point of symmetry is now seen to occur at $\theta_1 = 180.0°$. The lowest energy structure in the case when $\theta_2 = 0.0°$ occurs at (75.0°, 0.0°) and is calculated to be -169.0907057 hartrees. Optimizing θ_1 and θ_2 at this point results in a stationary point that occurs at (73.23°, 0.0°) and is identified as the global minimum.

We now demonstrate that a surface fit of the energy leads to a situation in which the surface topology is well approximated. To this end, other points on the potential energy surface were generated by repeating the calculations for cases in which θ_2 was increased by increments of 60.0° while θ_1 was made to span the range 0.0° to 360.0° in 5.0° increments for a given θ_2. A similar strategy was used by fixing θ_1 and incrementing θ_2. The totality of the points were then fitted on a surface equation using the program STEPWISE. In order to increase the accuracy of the fits, -169.00 hartrees were subtracted from each energy value, which were then multiplied by 100. In Table 1 we report the 26 terms that were necessary to fit the surface to within a tolerance of 0.0001 hartrees. The difference in the fitted energy for a given conformer at the point (θ_1, θ_2) and the fitted energy of the global minimum is then determined and plotted as a two-dimensional topological surface (Fig. 2). The various stationary points identified in Fig. 2, which must be interpreted as starting values for the true critical points on the potential energy surface of aminomethanol, have been determined by using program VA05 and the fitted equation. The symmetry of the topological surface clearly indicates a center of inversion around the point (180.0°, 180.0°).

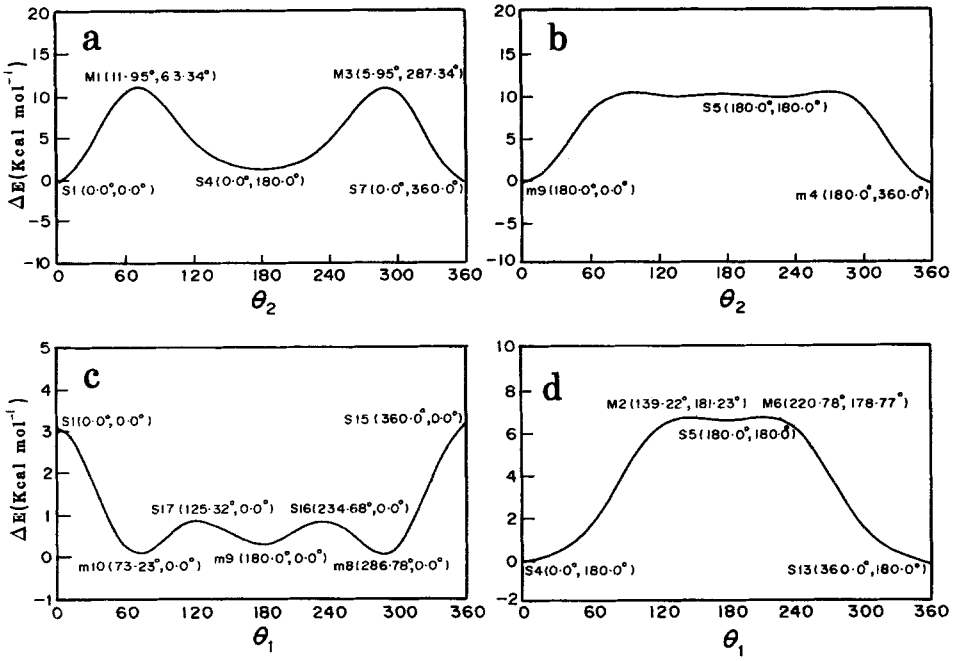

Fig. 1a–d. The difference in the 3-21G energy from the lowest energy structure in kcal/mol vs the dihedral angle. **a** $\theta_1 = 0.0°$; **b** $\theta_1 = 180.0°$; **c** $\theta_2 = 0.0°$; **d** $\theta_2 = 180.0°$. The GAUSSIAN88 stationary points are shown in the figure

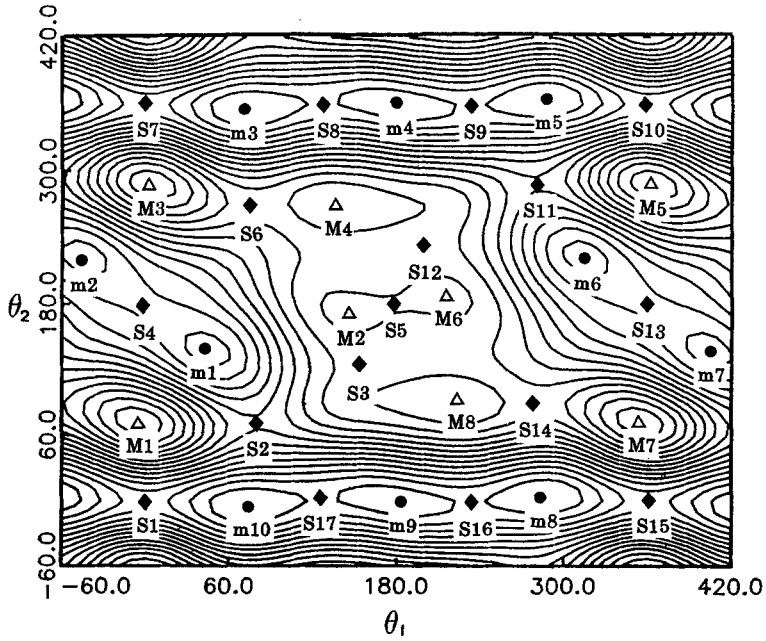

Fig. 2. A two-dimensional topological surface for the (θ_1, θ_2) system in accordance with the fitted equation. The stationary points on the surface are indicated by *m*, *M* and *S* for minima (●) maxima (△) and transition states (◆) (first order saddle points) respectively

Table 1. The terms in the fitted surface equation for θ_1 and θ_2 rotations. The equation was obtained after subtracting -169.00 hartrees from the energy values. The value of the constant (cf. Eq. (1)) is $k = -7.900896$

Term	c_i	f_{1i}	f_{2i}
1	−0.32803187	1.0	$\cos(\theta_2)$
2	−0.46294194	1.0	$\cos(2\theta_2)$
3	−0.23530788	1.0	$\cos(3\theta_2)$
4	−0.22786260	$\sin(\theta_1)$	$\sin(\theta_2)$
5	0.10809006	$\sin(\theta_1)$	$\sin(2\theta_2)$
6	0.04516525	$\sin(\theta_1)$	$\sin(3\theta_2)$
7	−0.07629486	$\sin(2\theta_1)$	$\sin(\theta_2)$
8	0.12830789	$\sin(2\theta_1)$	$\sin(2\theta_2)$
9	0.02423141	$\sin(2\theta_1)$	$\sin(3\theta_2)$
10	−0.01890477	$\sin(3\theta_1)$	$\sin(\theta_2)$
11	−0.01946518	$\sin(3\theta_1)$	$\sin(4\theta_2)$
12	−0.11238490	$\cos(\theta_1)$	1.0
13	0.42004048	$\cos(\theta_1)$	$\cos(\theta_2)$
14	−0.11571937	$\cos(\theta_1)$	$\cos(2\theta_2)$
15	−0.06658958	$\cos(\theta_1)$	$\cos(3\theta_2)$
16	−0.00992300	$\cos(\theta_1)$	$\cos(4\theta_2)$
17	0.12845524	$\cos(2\theta_1)$	1.0
18	0.12438384	$\cos(2\theta_1)$	$\cos(\theta_2)$
19	−0.10849206	$\cos(2\theta_1)$	$\cos(2\theta_2)$
20	−0.03367410	$\cos(2\theta_1)$	$\cos(3\theta_2)$
21	0.11435371	$\cos(3\theta_1)$	1.0
22	0.02178989	$\cos(3\theta_1)$	$\cos(\theta_2)$
23	−0.02026804	$\cos(3\theta_1)$	$\cos(2\theta_2)$
24	−0.01082623	$\cos(3\theta_1)$	$\cos(3\theta_2)$
25	0.01038196	$\cos(4\theta_1)$	1.0
26	−0.00796084	$\cos(4\theta_1)$	$\cos(4\theta_2)$

In Fig. 3, a two-dimensional topological map shows the various paths that connect minima with transition states. The *ab initio* energy difference of each point (in kcal/mol) relative to the global minimum is also shown in the figure. Points that are symmetry equivalent naturally have the same ΔE values. The global maximum is seen to occur at an energy of 14.13 kcal/mol relative to the global minimum. The description of each of the critical points is summarized in Table 2, together with the *ab initio* energy difference from the lowest energy structure (kcal/mol) and the corresponding total energy in hartrees; asterisks indicate points that are symmetry equivalent to other points.

2.2. *The* (θ_1, γ) *surface*

Details of the surface equation for the (θ_1, γ) system are summarized in Table 3. Since the θ_1 function includes only cosine terms, the system as a whole is expected to exhibit reflective symmetry around the $\theta_1 = 180.0°$ axis. This symmetry may be verified by inspecting Fig. 4, which is a three-dimensional representation of the surface topology. Table 4 is analogous to Table 2, and lists all the

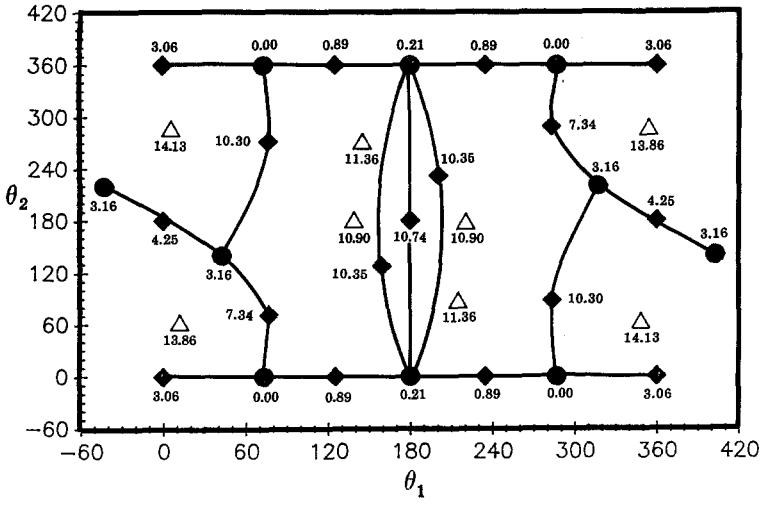

Fig. 3. A two-dimensional topological map showing the stationary points for the (θ_1, θ_2) surface of the rigid rotor. The values in the figure indicate the difference in energy (kcal/mol) from the lowest energy structure. Paths that connect transition states (first order saddle points) with minima are indicated. Symbols as for Fig. 2

critical points involved in the (θ_1, γ) system. The points $S4$ (0.0°, 180.0°) on the (θ_1, θ_2) surface should in fact be equivalent to the point $S1$ (0.0°, 120.0°) on the (θ_1, γ) surface in which $\theta_2 = 0.0°$. Although these points had been identified as transition states, they are not equivalent since in the (θ_1, γ) system, the stationary point occurs at $\gamma = 125.69°$ rather than 120.0°. These points, however, should be very close to a stationary point on the hypersurface defined by the three angles and the difference in their energy is $\cong 1$ kcal/mol. In Fig. 5 we show ball and stick models of the different transition states (first order saddle points). In these figures, the highest component vectors associated with the negative frequency are superposed on the diagram. These vectors indicate the forces acting on the molecule trying to pull it away from the transition state.

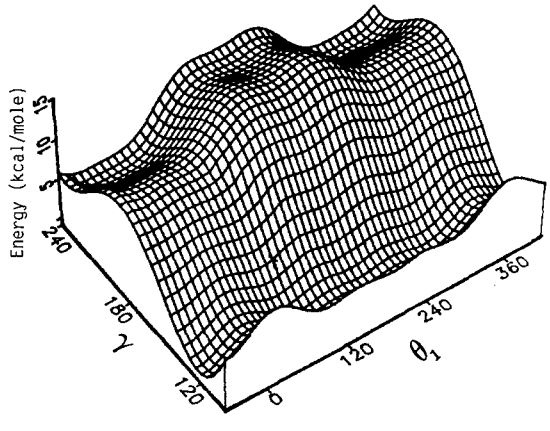

Fig. 4. A three-dimensional topological surface for the (θ_1, γ) system in accordance with the fitted equation. Energy differences from the zero point energy are in kcal/mol

Table 2. Stationary points identified as minima, transition states and maxima obtained by the GAUSSIAN88 package (Opt) and by program VA05 (Fit) for the (θ_1, θ_2) conformers. Points marked by an asterisk are the unique points. The set of equivalent points may be determined by comparing the difference in the energy of these points from the energy of the global minimum (ΔE in kcal/mol). The global minimum is the point that corresponds to a $\Delta E = 0.00$ kcal/mol

Minima					
Type	θ_1 (°)	θ_2 (°)	Point	Energy (hartrees)	ΔE (kcal/mol)
Opt	−42.92	219.79	*m2	−169.0856716	3.16
Fit	−44.55	222.44			
Opt	73.23	0.00	m10	−169.0907057	0.00
Fit	74.15	0.00			
Opt	180.00	0.00	m9	−169.0903680	0.21
Fit	180.00	0.00			
Opt	286.78	0.00	*m8	−169.0907057	0.00
Fit	285.85	0.00			
Opt	42.92	140.21	m1	−169.0856716	3.16
Fit	44.55	137.56			
Opt	317.08	219.79	*m6	−169.0856716	3.16
Fit	315.45	222.44			
Opt	73.23	360.00	*m3	−169.0907057	0.00
Fit	74.15	360.00			
Opt	180.00	360.00	*m4	−169.0903680	0.21
Fit	180.00	360.00			
Opt	286.78	360.00	*m5	−169.0907057	0.00
Fit	285.85	360.00			
Opt	402.92	140.21	*m7	−169.0856716	3.16
Fit	404.55	137.56			
Transition states					
Opt	0.00	0.00	S1	−169.0858331	3.06
Fit	0.00	0.00			
Opt	0.00	180.00	S4	−169.0839395	4.25
Fit	0.00	180.00			
Opt	0.00	360.00	*S7	−169.0858331	3.06
Fit	0.00	360.00			
Opt	125.32	0.00	S17	−169.0892950	0.89
Fit	125.99	2.77			
Opt	234.68	0.00	*S16	−169.0892950	0.89
Fit	234.01	2.77			
Opt	360.00	0.00	*S15	−169.0858331	3.06
Fit	360.00	0.00			
Opt	180.00	180.00	S5	−169.0735930	10.74
Fit	180.00	180.00			
Opt	77.02	71.21	S2	−169.0790060	7.34
Fit	79.84	70.89			
Opt	76.53	271.78	S6	−169.0742978	10.30
Fit	78.75	270.34			

Table 2 (continued)

Transition states					
Opt	159.13	128.30	*S*3	−169.0742185	10.35
Fit	165.22	128.34			
Opt	125.32	360.00	**S*8	−169.0892950	0.89
Fit	125.99	360.00			
Opt	234.68	360.00	**S*9	−169.0892950	0.89
Fit	234.01	360.00			
Opt	360.00	360.00	**S*10	−169.0858331	3.06
Fit	360.00	360.00			
Opt	282.98	288.70	**S*11	−169.0790060	7.34
Fit	280.16	289.11			
Opt	283.47	88.22	**S*14	−169.0742978	10.30
Fit	281.25	89.66			
Opt	200.87	231.70	**S*12	−169.0742185	10.35
Fit	194.78	231.66			
Opt	360.00	180.00	**S*13	−169.0839395	4.25
Fit	360.00	180.00			
Maxima					
Opt	11.95	63.34	*M*1	−169.0686215	13.86
Fit	4.65	72.57			
Opt	5.95	287.34	*M*3	−169.0681891	14.13
Fit	4.65	287.44			
Opt	139.22	181.23	*M*2	−169.0733408	10.90
Fit	141.66	174.09			
Opt	145.12	272.14	*M*4	−169.0726086	11.36
Fit	135.97	270.76			
Opt	214.88	87.86	**M*8	−169.0726086	11.36
Fit	224.04	89.24			
Opt	220.78	178.77	**M*6	−169.0733408	10.90
Fit	218.34	185.91			
Opt	348.05	63.34	**M*7	−169.0681891	14.13
Fit	355.35	72.56			
Opt	354.05	287.34	**M*5	−169.0686215	13.86
Fit	355.35	287.43			

2.3. The fitted equations

The fitted (Fit) and optimized (Opt) structures reported in Tables 2 and 4 are seen to correlate very well especially in cases where the system exhibits symmetry around at least one coordinate. The surface defined by the (θ_1, θ_2) angles, however, is more complex because of the center of inversion around the (180.0°, 180.0°) point. The vectors that define the fitted functions (Table 1) should, therefore, include both sine and cosine terms. It is also apparent that if

Table 3. The terms in the fitted surface equation for θ_1 and γ rotations. The equation was obtained after subtracting -169.00 hartrees from the energy values. The value of the constant (cf. Eq. (1)) is $k = -3.07467009$

Term	c_i	f_{1i}	f_{2i}
1	−0.17959624	1.0	$\cos(\theta_1)$
2	0.09109161	1.0	$\cos(3\theta_1)$
3	−0.64691339	$\sin(\gamma)$	1.0
4	0.40963205	$\sin(\gamma)$	$\cos(\theta_1)$
5	0.10541264	$\sin(\gamma)$	$\cos(2\theta_1)$
6	−0.03139039	$\sin(3\gamma)$	1.0
7	7.31012669	$\cos(\gamma)$	1.0
8	0.11537112	$\cos(\gamma)$	$\cos(\theta_1)$
9	3.27316718	$\cos(2\gamma)$	1.0
10	−0.04539434	$\cos(2\gamma)$	$\cos(2\theta_1)$

Table 4. Stationary points identified as minima, transition states and maxima obtained by the GAUSSIAN88 package (Opt) and by program VA05 (Fit) for the (θ_1, γ) conformers. Points marked by an asterisk are the unique points. The set of equivalent points may be determined by comparing the difference in the energy of these points from the energy of the global minimum (ΔE in kcal/mol). The global minimum is the point that corresponds to a $\Delta E = 0.0$ kcal/mol

Minima					
Type	θ_1 (°)	γ (°)	Point	Energy (hartrees)	ΔE (kcal/mol)
Opt	0.00	234.72	*m*3	−169.0843525	4.05
Fit	0.00	234.55			
Opt	72.23	122.52	*m*1	−169.0908022	0.00
Fit	69.32	123.13			
Opt	180.00	121.58	*m*2	−169.0904116	0.25
Fit	180.00	121.39			
Opt	180.00	232.55	*m*4	−169.0743263	10.34
Fit	180.00	233.16			
Opt	287.77	122.52	**m*6	−169.0908022	0.00
Fit	290.68	123.13			
Opt	360.00	234.72	**m*5	−169.0843525	4.05
Fit	360.00	234.55			
Transition states					
Opt	−31.45	183.52	**S*2	−169.0737777	10.68
Fit	−35.65	183.58			
Opt	0.00	125.69	*S*1	−169.0863456	2.80
Fit	0.00	125.70			
Opt	31.45	183.52	*S*2	−169.0737777	10.68
Fit	35.65	183.58			

Table 4 (continued)

Transition states					
Opt	125.34	121.38	*S*11	−169.0893287	0.92
Fit	118.92	120.96			
Opt	141.21	233.10	*S*4	−169.0738922	10.61
Fit	141.69	234.51			
Opt	180.00	190.83	*S*6	−169.0684957	14.00
Fit	180.00	190.91			
Opt	218.79	233.10	**S*5	−169.0738922	10.61
Fit	218.31	234.51			
Opt	234.66	121.38	**S*10	−169.0893287	0.92
Fit	241.08	120.96			
Opt	328.55	183.52	**S*7	−169.0737777	10.68
Fit	324.35	183.58			
Opt	360.00	125.69	**S*9	−169.0863456	2.80
Fit	360.00	125.70			
Opt	391.45	183.52	**S*8	−169.0737777	10.68
Fit	395.65	183.58			
Maxima					
Opt	0.00	181.77	*M*2	−169.0736577	10.76
Fit	0.00	181.85			
Opt	141.46	190.12	*M*1	−169.0677769	14.45
Fit	136.43	189.85			
Opt	218.54	190.12	**M*4	−169.0677769	14.45
Fit	223.57	189.85			
Opt	360.00	181.77	**M*3	−169.0736577	10.76
Fit	360.00	181.85			

one were to fix θ_2, the surface equation would include a Fourier series of the form:

$$E(\theta_1, \theta_2 = \text{constant}) = k + \sum_n a_n \cos(n\theta_1) + \sum_n b_n \sin(n\theta_1), \tag{8}$$

where k is a constant. In particular, if θ_1 is fixed at 0.0° or 180.0°, all terms that involve the sine of θ_1 vanish and one is left with a cross section of the surface that depends only on the cosine terms and which is symmetrical around the point $\theta_1 = 180.0°$. In regions in which θ_2 is chosen close to zero, sine terms in the $\langle f_2|$ vector appear and consequently there will be an immediate breakdown in the symmetry around the $\theta_1 = 180.0°$ point. The inversion properties of the surface are in fact dependent on the inclusion of sine terms in the energy expression. In cases where θ_2 is fixed at 90.0° or 270.0°, the contribution from the sine terms in θ_1 becomes most important and these are the points on the surface in which the system is expected to exhibit greatest deviation from symmetry around the $\theta_1 = 180.0°$ point. Similarly, it may be shown that a cross section in which $\theta_1 = 90.0°$ or 180.0° should produce points that are symmetrical around $\theta_2 = 180.0°$.

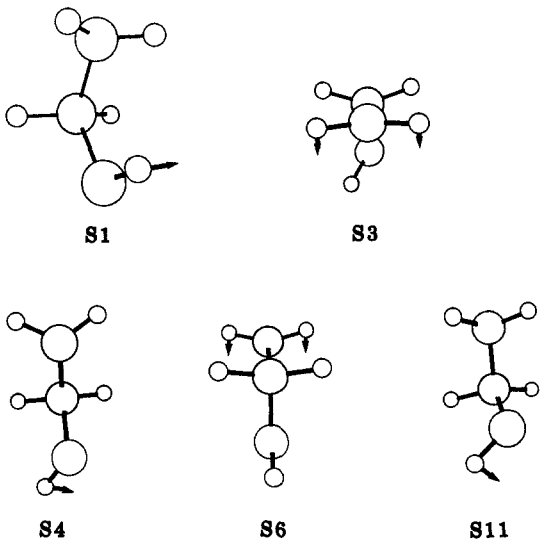

Fig. 5. Ball and stick models for the GAUSSIAN88 first order saddle points. The highest component vectors associated with the negative frequency are superposed on the diagrams

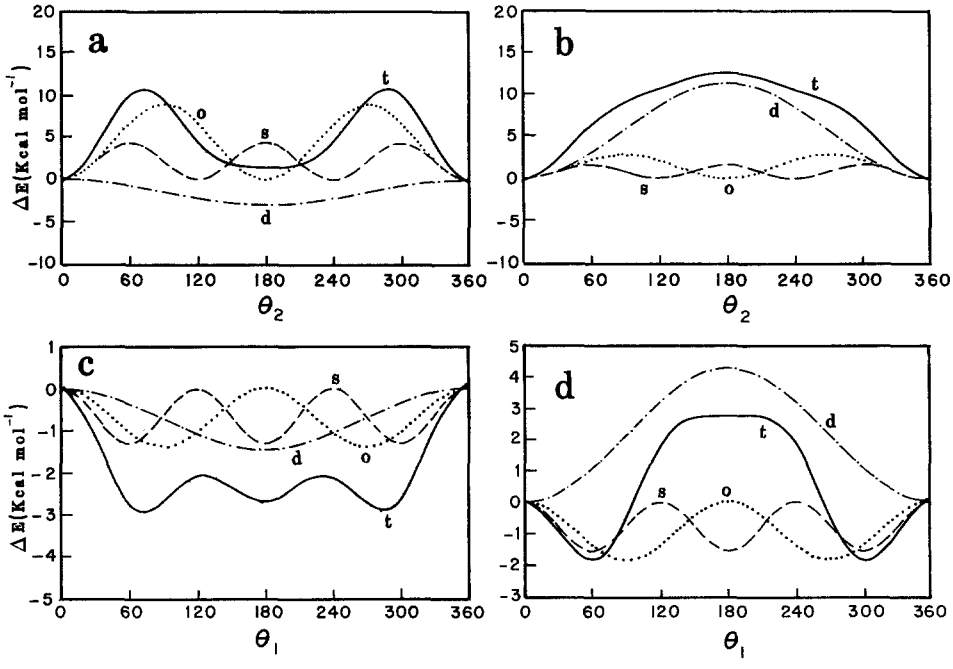

Fig. 6a–d. The deconvoluted fitted potential energy relative to a "zero point" energy (kcal/mol) in terms of the dipole (*d*), steric (*s*) and orthogonal (*o*) components for the (θ_1, θ_2) surface. The curve expressing the sum of these terms is indicated by (*t*) (solid line). **a** $\theta_1 = 0.0°$; **b** $\theta_1 = 180.0°$; **c** $\theta_2 = 0.0°$; **d** $\theta_2 = 180.0°$

In contrast, the (θ_1, γ) surface exhibits symmetry along the cross section in which $\theta_1 = 180.0°$. This is apparent since the θ_1 dependence involves only cosine terms and for a given γ, the surface equation would assume the form:

$$E(\theta_1, \gamma = \text{constant}) = k' + \sum_n a_n \cos(n\theta_1). \tag{9}$$

However, since fixing θ_1 would produce an equation that involves both the sines and cosines of γ, any section that crosses a given θ_1 is deemed to exhibit no symmetry properties. There is no doubt, therefore, that the fitted equation reproduces the symmetry properties of the surfaces in an unambiguous manner.

The only points on the surface in which the symmetry is not accurately reproduced are those very close to the transition state *S*5 (180.0°, 180.0°) on the (θ_1, θ_2) surface. The fitted equation predicts the two maxima *M*2 and *M*6 to occur at (141.66°, 174.09°) and (218.34°, 185.91°) respectively, in contrast with the optimized *ab initio* points that are found to have the coordinates (139.22°, 181.23°) and (220.78°, 178.77°), respectively. The line joining the points *M*2–*S*5–*M*6 is predicted to have a positive slope by the fitted equation, while the optimized results predict the sign of the slope to be negative. It may be pointed out, however, that the surface equation around the $\theta_2 = 180.0°$ axis includes very small contributions from sine terms in θ_2 and are subject to relatively large errors. Including more points around this axis would most definitely improve the fitted equation, but this is not necessary since the general features of the topological surface are accurately reproduced even without these points.

2.4. The deconvolution of the potential energy

We shall now demonstrate that the surface equation can be used to describe the various potential energy components that are associated with our model. In a manner similar to the one that had been described by Pople et al. for the methanediol model [20–22] we identify three such components, namely the steric, orthogonal and dipole factors. The steric factor favors a staggered conformation while the dipole factor favors a conformation in which the sp^3 hybridized lone pair on the nitrogen and the oxygen centers are such that one is periplanar while the other is antiperiplanar. The orthogonal component, however, favors a conformation in which the lone pair of electrons on the nitrogen and the lone pair of electrons in the 2*p*-type orbital of oxygen are contained in the N–C–O plane. These factors are summarized in Diagrams 2–4.

We now consider the (θ_1, θ_2) fitted equation in which θ_1 is chosen to be zero (Table 1). Since all terms in sine of θ_1 are coupled with terms in sine of θ_2, the equation along this cross section reduces to one that has a functional dependence on $\cos(n\theta_2)$ [$n = 1$, 2, 3 and 4]. This equation may be rearranged to give

$$E(\theta_2) = k + V_d(1 - \cos\theta_2) + V_o(1 - \cos 2\theta_2) + V_s(1 - \cos 3\theta_2), \tag{10}$$

in which $V_d = 1.49$ kcal/mol, $V_o = -4.44$ kcal/mol and $V_s = -2.17$ kcal/mol, and k may be identified as a "zero point" energy, $E_0(\theta_2)$. A plot of ΔE ($\equiv E_0(\theta_2) - E(\theta_2)$) vs θ_2 is therefore the fitted counterpart of the rigid rotor *ab initio* model given in Fig. 1a. This difference is plotted in Fig. 6a (solid line) together with the deconvoluted components. It is interesting to note that the above equation naturally arises from the fitted equation and is identical to the

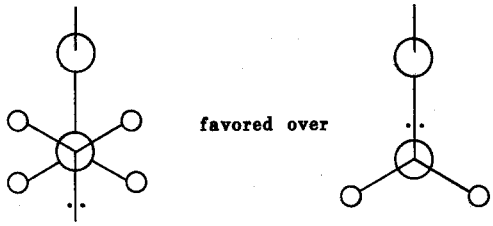

Diagram 2. Steric component

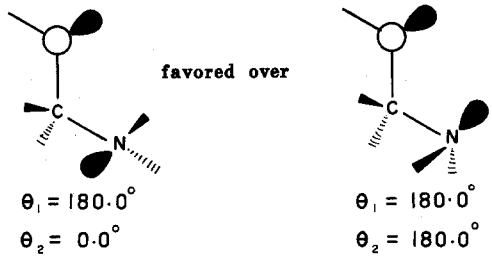

Diagram 3. Dipole component

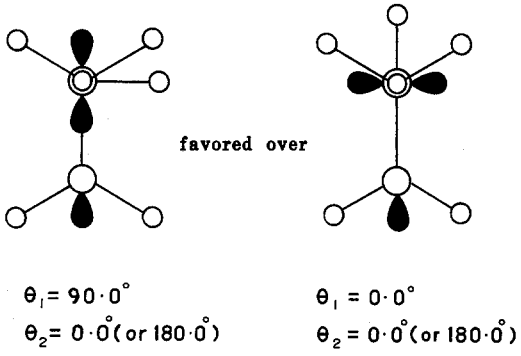

Diagram 4. Orthogonal component

one that had been empirically suggested by Pople. The term that involves $(1 - \cos\theta_2)$ exhibits a minimum at 180.0° and may be identified with the dipole-dipole component (V_d) of the potential energy in which $2V_d$ is the stabilization energy associated with the antiperiplanar-periplanar conformer compared with the antiperiplanar-antiperiplanar conformer. The term that involves $(1 - \cos 2\theta_2)$, on the other hand, exhibits a maximum at 90.0° and is essentially the orthogonal component (V_o); it involves a stabilization energy of 8.88 kcal/mol in which the sp^3 hybridized orbitals on N and the $2p$-type orbital

O are contained in the N–C–O plane. These factors are associated with the "anomeric" effect [23–25] and may be rationalized by the partial withdrawal of charge from the $2p$-type orbital on C towards the C–N bond which is apparently enhanced when the $2p$-type lone pair of electrons on O are *staggered* with respect to $-CH_2$ (Diagram 4). The anomeric effect is responsible for the relative stability of α-anomers with respect to the β-anomers in hexoses (except for glucose) [26]. In the former anomer, the dipoles between the ring oxygen and the axial hydroxyl groups are antiparallel and this is favored over the case in which the dipoles are parallel, as in the β-anomer. Finally, the steric factors (V_s) (Diagram 2) are expected to favor a staggered over an eclipsed conformation and involve a destabilization energy of 4.34 kcal/mol at an angle of $\theta_2 = 60.0°$. An equation similar to Eq. (10) ensues upon fixing θ_1 at 180.0° (Fig. 6b). Although the steric and orthogonal factors are reproduced in sense, the relative magnitude of the V_s and V_o terms are seen to be reduced by almost (1/3). The dipole factor, however, is seen to change dramatically in both sense and relative magnitude and is maximum when $\theta_2 = 180.0°$. This may be attributed to the fact that the conformer in which the lone pair of electrons on the N and O are both periplanar is greatly destabilized.

A surface equation that has functional dependence on $\cos(n\theta_1)$ may be obtained by fixing θ_2 to 0.0° or 180.0°, as may be verified by inspecting Table 1. The plot shown in Fig. 6c includes the zero point destabilization energy (solid line) and the deconvoluted terms in the case when $\theta_2 = 0.0°$. The dipole contribution to the potential energy is similar to that in Fig. 6a, and this is expected since the point $\theta_2 = 180.0°$ corresponds to the case in which the lone pair of electrons on the N atom are antiperiplanar whereas those on the O atom are periplanar. The phase shift of 60.0° in the steric factor relative to that in Fig. 6a is attributed to the fact that the alcoholic hydrogen is sterically hindered at $\theta_1 = 0.0°$ due to its proximity to the amino group and favors a conformation in which $\theta_1 = 60.0°$ or 180.0°. The 90.0° phase shift in the orthogonal component is similar to the one that had been reported by Pople et al. and is seen to favor a conformation in which $\theta_1 = 90.0°$ (see Diagram 4). The case in which θ_2 is fixed at 180.0° (Fig. 6d) reproduces the orthogonal and steric components but, as expected, the dipole component is seen to behave in a manner similar to that depicted in Fig. 6b.

For the (θ_1, γ) surface equation (Table 3), we note that fixing θ_1 would reduce to an equation that involves both sines and cosines of γ. This would naturally lead to a situation in which antisymmetric terms around the point $\gamma = 180.0°$ (sines of γ) are superposed on symmetric terms (cosines of γ). We also note that the fitted equation in which γ is fixed at 120.0° and θ_1 is allowed to change (Fig. 7a) should be identical in describing the topology of that cross section to the case when $\theta_2 = 0.0°$ and θ_1 is allowed to vary (Fig. 6c). The two fitted equations are therefore capable of describing the same cross section from two different perspectives. The accuracy in reproducing the topology of the cross section is, to say the least, remarkable and the deconvoluted components, V_d, V_o and V_s, come out to be 0.72, 0.69 and 0.66 kcal/mol, respectively, in the (θ_1, θ_2) equation compared with 0.74, 0.72 and 0.57 kcal/mol in the (θ_1, γ) equation.

The case in which γ is fixed at 180.0° (Fig. 7b) is of special interest since it represents a situation in which the coordination around the N atom is forced into sp^2 hybridization. The lone pair of electrons are in fact forced to occupy a local non-hybridized orbital and consequently a rotation of θ_1 by 90.0° would result in having this orbital and the sp^3 hybridized orbital on the N atom to be

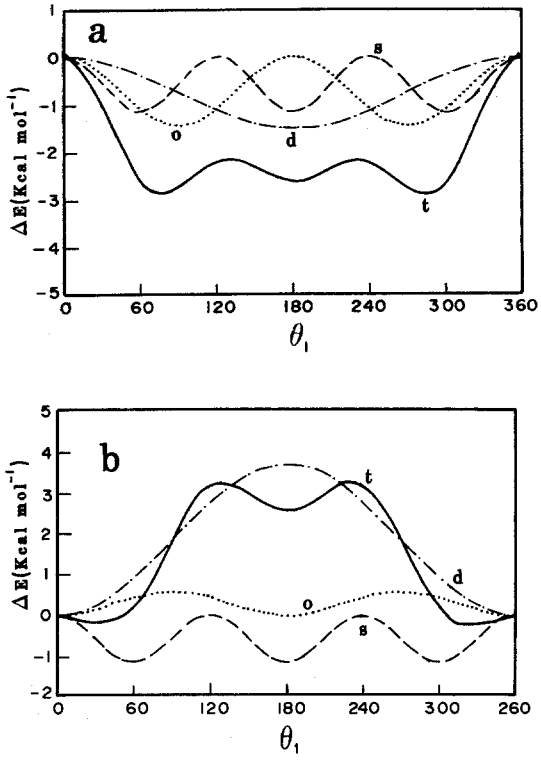

Fig. 7a,b. The deconvoluted fitted potential energy relative to a "zero point" energy (kcal/mole) in terms of the dipole (*d*), steric (*s*) and orthogonal (*o*) components for the (θ_1, γ) surface. The curve expressing the sum of these terms is indicated by (*t*) (solid line). **a** $\gamma = 120.0°$; **b** $\gamma = 180.0°$

contained in the N–C–O plane with a relative destabilization. The behavior of the steric and dipole factors, however, follows expected trends and must be compared with such trends in Fig. 6d. In particular, it may be noted that the combined stabilization of the steric and orthogonal factors are responsible for the local minimum in the total energy that appears at an angle of $\theta_1 = 180.0°$ (compare, for instance, this point with a similar point in Fig. 6d).

As has been mentioned earlier, the unsymmetric representation of the potential energy around the point $\gamma = 180.0°$ is manifested by the inclusion of both, sine and cosine terms in γ in the fitted equation when θ_1 is fixed. In this case, the components in the potential energy expression would involve only steric and dipole terms. The $\gamma = 120.0°$ case corresponds to the staggered conformer while the eclipsed conformer is obtained when γ assumes the value of 240.0°, and the apparent stability of the staggered conformer can best be described by a term that carries a functional dependence on $-\sin\gamma$. The "dipole factor", however, is a compound term involving $\sin(n\gamma)$ and $\cos(n\gamma)$ and cannot be factored out in a manner that would allow one to explain unambiguously the preferred antiperiplanar-antiperiplanar conformation. We also note that it is not possible to define a single point reference (a "zero point" energy for instance) as in the previous cases. This term is actually contaminated with other terms that involve the interaction of the electron pairs on the N and O atoms during the inversion process.

In Table 5, we summarize the cross-sectional equations for the cases that had been discussed so far. Our results are in excellent qualitative agreement with results that had been reported for the methanediol model [20]. Results that had been reported on aminomethanol by Radom et al. [22] and by Kaliannan et al.

Table 5. Dipole (V_d), orthogonal (V_o) and steric (V_s) components of the potential energy surfaces for the different cross sections as determined by θ_1, θ_2 and γ. Energy is in kcal/mol

	V_d	V_o	V_s
$\theta_1 = 0.0°$			
$E(\theta_2) = k$	$+1.49(1-\cos\theta_2)$	$-4.44(1-\cos 2\theta_2)$	$-2.17(1-\cos 3\theta_2)$
$\theta_1 = 180.0°$			
$E(\theta_2) = k$	$-5.61(1-\cos\theta_2)$	$-1.37(1-\cos 2\theta_2)$	$-0.78(1-\cos 3\theta_2)$
$\theta_2 = 0.0°$			
$E(\theta_1) = k$	$+0.72(1-\cos\theta_1)$	$+0.69(1-\cos 2\theta_1)$	$+0.66(1-\cos 3\theta_1)$
$\theta_2 = 180.0°$			
$E(\theta_1) = k$	$-2.13(1-\cos\theta_1)$	$+0.92(1-\cos 2\theta_1)$	$+0.78(1-\cos 3\theta_1)$
$\gamma = 120.0°$			
$E(\theta_1) = k$	$+0.74(1-\cos\theta_1)$	$+0.72(1-\cos 2\theta_1)$	$+0.57(1-\cos 3\theta_1)$
$\gamma = 180.0°$			
$E(\theta_1) = k$	$-1.85(1-\cos\theta_1)$	$-0.28(1-\cos 2\theta_1)$	$+0.57(1-\cos 3\theta_1)$

[27] are also in excellent qualitative agreement. The only problem with the results reported in the Kaliannan paper is that the torsional angles were incremented by 60.0° and no attempt was made to identify the local and the global minima properly. For instance, the conformer in which $\theta_2 = 0.0°$ and $\theta_1 = 60.0°$ was assumed to be a stationary point and no attempt was made to study this cross section in greater detail. This point is indeed stationary from a "steric" point of view but, according to our results, the inclusion of the orthogonal and dipole terms causes the θ_1 angle to shift to a favored value of 73.23°. The staggered and eclipsed conformers in cases where the dipole and anomeric effects are absent (ethane for example) are definitely expected to be stationary, and torsional angular increments by 60.0° would likewise produce stationary points on the surface. The points that had been used in that study do not seem to be enough to reproduce the details of the surface, and their method of identifying the stabilization and destabilization energies of the various components is arbitrary and is based on the early work of Pople. It is unfortunate that no quantitative comparison can be made since the reference points used in evaluating the potential energy component are is not identical to those used in our calculations.

The conclusion to be drawn from this is that our model predicts the path *m*10–*S*17–*m*9–*S*16–*m*8 (see Fig. 2) to involve small energy barriers and therefore that the hydroxyl hydrogen is subject to almost free rotation around the C–O axis. This confirms the conclusion arrived at by Kaliannan and co-workers regarding aminomethanol and aminosulfonic acid. However, in order to qualify this conclusion further, rigorous fully relaxed 6-31G* calculations were performed in order to identify these points and the corresponding energy barriers associated with this path correctly.[1]

[1] We do not report the fully optimized geometry of all of these points since this is not relevant to our discussion. The two dihedral angles of interest remain to be θ_1 and θ_2. The reference to θ_2 throughout the paper is the angle that the vector perpendicular to that defining the lone pair of electrons on N makes with the N–C–O plane and is actually measured relative to the two dihedral angles that the amino hydrogens make with the same plane.

The fully optimized 6-31G* global minimum ($m10$, Fig. 2) occurs at an angle of $\theta_1 = 69.48°$, the dihedral angles defining the amino hydrogens being $-53.85°$ and 66.41°. The optimized energy at this point is -170.068356428 hartrees. The structures defined by the points $S1$ and $m9$ have both C_s symmetry and are correctly identified as a transition state and a local minimum, respectively, having energies of -170.06451684 hartrees and -170.068135231 hartrees. The structure defined by the point $S17$ was first obtained by optimizing the geometry at $\theta_1 = 125.0°$ followed by a fully relaxed search of the transition state using the OPT = (TS, CALCFC) keyword. The energy associated with this point is calculated to be -170.066553530 hartrees and occurs at an angle $\theta_1 = 124.36°$, the dihedral angles defining the amino hydrogens being $-60.26°$ and 57.67°. The fully relaxed 6-31G* energy differences (in kcal/mol) relative to the global minimum along the path $m10$–$S17$–$m9$–$S16$–$m8$ are therefore 0.00, 1.13, 0.14, 1.13 and 0.00, and should be compared with the values reported in Fig. 3 for the

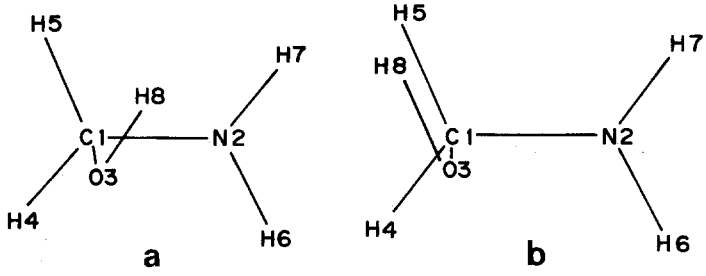

Fig. 8. 6-31G* fully optimized structure of the global minimum ($m10$) and the transition state $S17$ on the (θ_1, θ_2) surface. Dihedral anticlockwise rotation is positive and rotational axis defined by the second and third atoms

a Structure of $m10$
Distances (Å)
C1N2 = 1.4329 C1O3 = 1.4039 C1H4 = 1.0795 C1H5 = 1.0852
N2H6 = 1.0017 N2H7 = 1.0019 H8O3 = 0.9474

Angles (degrees)
O3C1N2 = 115.5976 H4C1N2 = 108.6648 H5C1N2 = 108.1997
H6N2C1 = 110.6192 H7N2C1 = 111.9469 H8O3C1 = 109.7832

Dihedral angles (degrees)
H4C1N2O3 = −118.0718 H5C1N2O3 = 124.4924
H6C1N2O3 = −53.8505 H7C1N2O3 = 66.4068
H8O3C1N2 = 69.4821

b Structure of $S17$
Distances (Å)
C1N2 = 1.4294 C1O3 = 1.4095 C1H4 = 1.0825 C1H5 = 1.0844
N2H6 = 1.0020 N2H7 = 1.0021 H8O3 = 0.9453

Angles (degrees)
O3C1N2 = 113.2320 H4C1N2 = 108.1378 H5C1N2 = 108.5294
H6N2C1 = 110.1440 H7N2C1 = 110.3986 H8O3C1 = 110.6529

Dihedral angles (degrees)
H4C1N2O3 = −120.1401 H5C1N2O3 = 112.7115
H6C1N2O3 = −60.2639 H7C1N2O3 = 57.6655
H8O3C1N2 = 124.3596

same path. The small energy barriers along this path support the results presented earlier in that the hydroxyl hydrogen is subject to almost free rotation along that path. It is also of interest to point out that the fitted equations of the rigid rotor model have identified these points correctly, and that the dihedral angle defining the hydroxyl hydrogen for the structures defining the points $m10$ and $S17$ are close to the 6-31G* fully relaxed values, namely 74.15° and 125.32° for the rigid rotor model compared with the respective values of 69.48° and 124.36° for the 6-31G* fully relaxed model. The fully optimized structures of the points $m10$ and $S17$ are shown in Fig. 8.

There is no doubt that the model that has been used in this work is simplified by assuming a rigid rotor and it is hoped that the reader will give more weight to the quality of the surface fits. Studies of surface fitting equations for fully relaxed and rigid rotor models at both the 4-31G and the 6-31G* level of approximation are in progress for methanediol and fluoroethanol [28]. Preliminary results suggest that the general topological features of the surfaces for a rigid rotor model are retained in a fully relaxed model, while the details of the surface in relation to the type and the geometry of the stationary points are subject to expected deviations. Global minima, however, are reproduced with reasonable accuracy. In the case of methanediol studied at the 4-31G level of approximation, for instance, the fitted equations of the rigid rotor model predict the global minimum to correspond to a synclinal-synclinal conformer in which the dihedral angles defining the hydroxyl hydrogens are (−64.82°, 63.81°) compared with the GAUSSIAN88 values of (−63.13°, 63.13°). This compares favorably with the fully relaxed values of the same model in which the fitted equations predict this point to occur at (−60.00°, 60.00°) compared with the GAUSSIAN88 values of (−62.07°, 62.07°). We point out, however, that in these calculations, the structure of methanediol was first optimized at the conformer in which the aforementioned dihedral angles were both fixed at 0.00°.

The present work, therefore, should not be mistaken for a representation of the fully optimized stationary points on the aminomethanol surface, but rather is a demonstration of the use of surface fitting equations in identifying stationary points on a topological surface.

Acknowledgements. The authors would like to express their gratitude to Professor Imre Csizmadia and Dr. Mike Peterson of the Chemistry Department, University of Toronto, for very fruitful discussions. The latter is also acknowledged for kindly providing us with programs STEPWISE and VA05. Credit is also due to Dr. Hamdy Nasserldine and Mrs Roula Abu Deheir of the Academic Scientific Department at the Kuwait University Computer Services for the installation and the initial testing of GAUSSIAN88. This work was supported by the Research Management Unit, Kuwait University (Projects SC044 and RMU041).

References

1. Murrell JN, Laidler KJ (1967) Trans Farad Soc 64:371
2. Peterson MR, Csizmadia IG (1982) In: Csizmadia IG (ed) Progress in theoretical organic chemistry: molecular structure and conformation. Recent advances, vol. 3. Elsevier, Amsterdam, p 190
3. Pavne PW, Allen LC (1977) In: Schaefer III HF (ed) Modern theoretical chemistry, vol. 4. Plenum Press, New York, p 29
4. Csizmadia IG (1989) In: Bartran J, Csizmadia IG (eds) New theoretical concepts for understanding organic reactions. Kluwer, London New York, p 1

5. Dewar MJS, Ford GP (1979) J Am Chem Soc 101:5558
6. Halgren TA, Kleier DA, Hall Jr JH, Brown LD, Lipscomb WN (1978) J Am Chem Soc 100:6595
7. Feller D, Bordon WT, Davidson ER (1979) J Chem Phys 70:4987
8. Draper NR, Smith H (1966) Applied regression analysis. Wiley, New York
9. Schlegel HB (1987) In: Lawley KP (eds) Ab initio methods in quantum chemistry–I. Wiley, New York, p 249
10. Fletcher R, Powell MJD (1963) Comput J 6:163
11. Murtagh BA, Sargent RWH (1972) Comput J 13:185
12. Fletcher R, Reeves CM (1964) Comput J 7:149
13. Frisch MJ, Head-Gordon M, Schlegel HB, Raghavachari K, Binkley JS, Gonzalez C, Derfees DJ, Fox DJ, Whiteside RA, Seeger R, Melius CF, Baker J, Martin R, Kahn LR, Stewart JJP, Fluder EM, Topiol S, Pople JA (1988) Gaussian, Inc, Pittsburgh, PA
14. Peterson MR (1989) Chemistry Department, University of Toronto, Canada
15. Powell MJD (1971) Subroutine VA05AD, AERE Harwell Subroutine Library, Harwell, Didcot, UK
16. Oosta GM, Gardner WT, Beeler DL, Rosenberg RD (1981) Proc Natl Acad Sci 78:829
17. Nordenman B, Bjork I (1981) Biochim Biophys Acta 672:227
18. Kaliannan B, Vishveshwara S, Rao VSR (1983) J Mol Struct 92:7
19. El-Issa (1990) Research Management Unit, Project RMU041, Kuwait University
20. Jeffrey GA, Pople JA, Radom L (1972) Carbohyd Res 25:117
21. Jeffrey GA, Pople JA, Binkley JS, Vishreshwara S (1978) J Am Chem Soc 100:373
22. Radom L, Hehre WJ, Pople JA (1971) J Am Chem Soc 93:289
23. Wolfe S, Rauk A, Tel LM, Csizmadia IG (1971) J Chem Soc (B) 136
24. Riddell FG (1967) Quart Rev 21:364
25. Eliel EL, Giza CA (1968) J Org Chem 33:3754
26. Rawn JD (1983) Biochemistry. Harper and Row, New York, p 277
27. Kaliannan P, Shveshwara SV, Rao VSR (1983) J Mol Struct (THEOCHEM) 105:359
28. El-Issa BD, Budeir RN (in progress)